

## Joints in the Mesozoic sediments around the Bristol Channel Basin

K. D. RAWNSLEY\*

Elf-Aquitaine, GTS, CSGGF, Avenue Laribatt, 64018 Pau, France

D. C. P. PEACOCK

Rock Deformation Research Group, School of Earth Sciences, University of Leeds, Leeds LS2 9JT, U.K.

T. RIVES

Elf-Aquitaine, GTS, CSGGF, Avenue Laribatt, 64018 Pau, France

and

J.-P. PETIT

Laboratoire de Géophysique et Tectonique, UMR 5573, Université Montpellier II, 34095, Montpellier Cedex 05, France

(Received 21 May 1997; accepted in revised form 11 June 1998)

**Abstract**—Analysis has been carried out at four locations on the edges of the Bristol Channel Basin to illustrate the later phases of deformation of a sedimentary basin, and to illustrate the control on joint patterns of subtle changes in the stress system. The characteristics of the joints are described and influences on joints are determined, including the roles of faults, folds and beds. There is a low coefficient of correlation between joint spacing and bed thickness, except in very thin limestone beds, which have a high density of joints. The lengths and spacings of earlier joint phases are usually greater than those of later phases. Later joints normally abut against earlier joints.

The joints abut the latest faults but are not displaced by them, so the joints post-date the main Alpine contraction. The joints formed in five main phases during reduction of the Alpine stresses. *Phase 1* joints are sub-parallel to the regional compression direction (160–180°). *Phase 2* joints are perturbed by faults, often curving towards points of stress concentrations along the faults. *Phase 3* joints are sub-parallel to the earlier E–W-striking fold axes. *Phase 4* joints are cross-joints, and *phase 5* joints form polygonal patterns within joint-bound blocks. Phases 2 and 3 do not occur in the absence of faults and folds, and correspond with a reduction in horizontal compression and an increase in the importance of local factors. Phases 4 and 5 occur at all locations. © 1998 Elsevier Science Ltd. All rights reserved

### INTRODUCTION

This paper illustrates the later phases of deformation of a sedimentary basin, and illustrates the importance of subtle changes in the stress system in causing joint patterns. The joint patterns at four extensive exposures of Triassic and Liassic sediments around the Bristol Channel Basin (BCB) are described. These locations (Fig. 1) are Sully Island (Long. 3°12'W, Lat. 51°24'N), Lavernock Point (Long. 3°10'W, Lat. 51°24'N), Nash Point (Long. 3°33'W, Lat. 51°24'N), and Lilstock (Long. 3°12'W, Lat. 51°12'N). The joint patterns that occur at these locations illustrate the variations in joints around the BCB. The BCB was chosen for study because of the extensive, excellent exposures, and because of the evidence present for the factors which influence joint development. The paper distils a large

amount of field observations, so some detail is inevitably lost.

The aims of this paper are to: (1) describe the joint patterns in the BCB, (2) show variabilities and similarities of joint patterns across the basin, and (3) interpret the development of the joints. Aerial photographs were taken from a helicopter from altitudes of a few tens of metres, and joint pattern characterization was undertaken using these high quality photographs. Scan-lines were used to quantify the joint patterns, both in the field and on the aerial photographs. For each of the four locations, the following is described: (1) geology, (2) joint characteristics, especially orientations, (3) interaction between joint sets, and (4) the effects of bedding planes, bed thickness, faults and folds. A local interpretation of joint origin is given, and information from the four locations is used to develop a regional model for joint development in the BCB. Such joint characteristics as spacings, lengths and apertures were measured (e.g. Rawnsley, 1990),

\*Now at BP Exploration, SPR, Chertsey Road, Sunbury-on-Thames TW16 7NE, U.K.

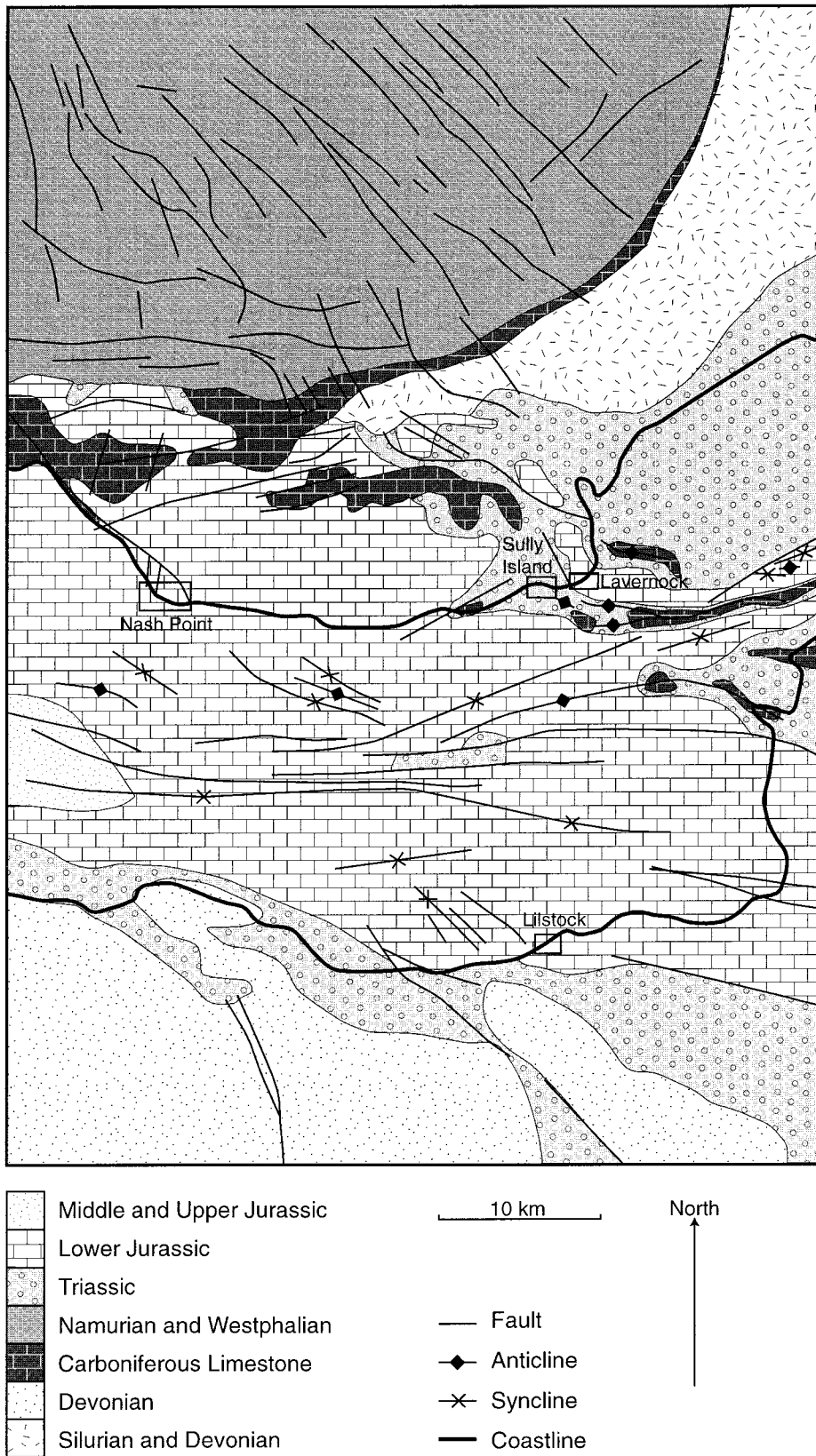


Fig. 1. Map showing the main geological features of the eastern Bristol Channel, with the positions of the locations studied. It is based on the Bristol Geological Survey sheet 51°N-04°W, Bristol Channel.

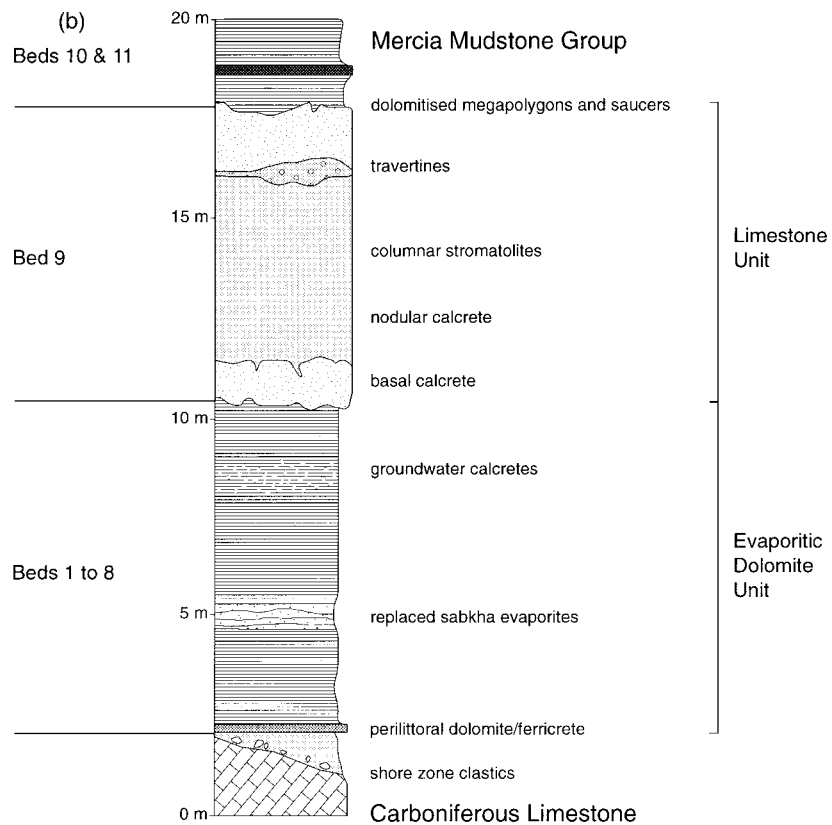
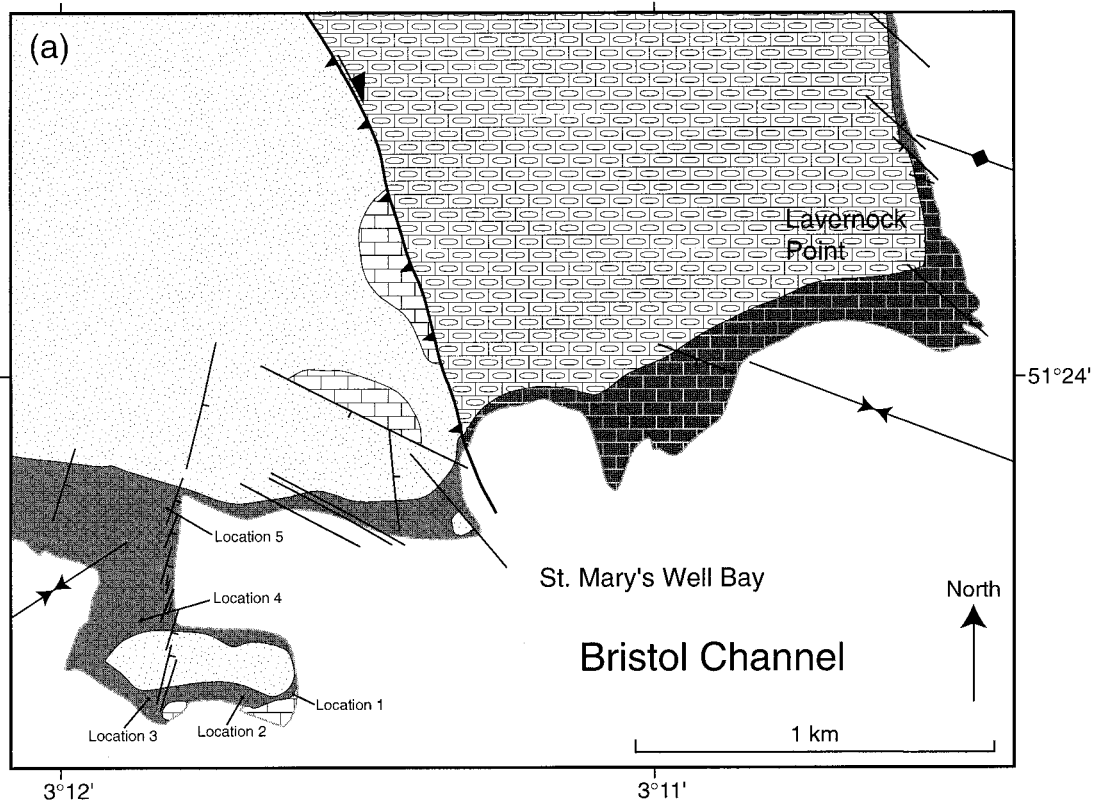


Fig. 2. (a) Geology and structure of the area between Sully Island and Penarth. (b) Sketch log of the succession of marginal lucustrine deposits exposed on the southern side of Sully Island.

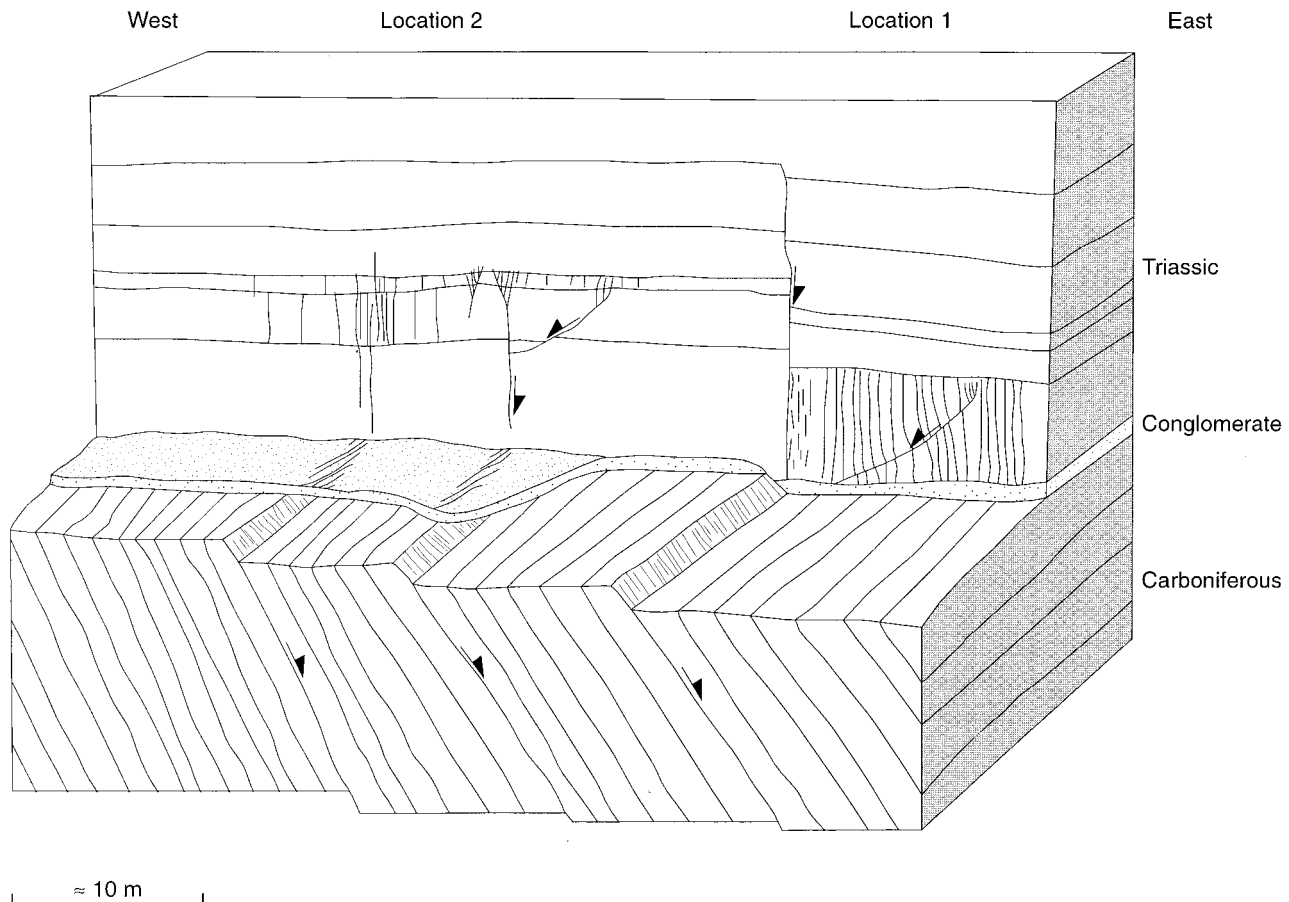


Fig. 3. Schematic view northwards of locations 1 and 2, Sully Island. Normal faulting along Carboniferous bedding planes produced faults and joints in the overlying Triassic sediments.

but the presentation of such data is not an aim of this paper.

In this paper, we discuss horizontal stresses, as does Hancock (1991). This is because stress refraction in the sub-horizontal beds means that the least compressive principal stress occurs approximately in the horizontal plane, with the orientations of the joints being controlled by the maximum ( $\sigma_H$ ) and least ( $\sigma_h$ ) horizontal stresses. It is the least compressive stress that is important in joint formation and propagation, with joints forming in effective tension (e.g. Engelder and Oertel, 1985). The joints in the Mesozoic sediments around the BCB are not mineralized and formed after the faults, which are mineralized. This implies that fluid pressure was less important during the joint formation than during the earlier faulting.

#### GEOLOGY OF THE BRISTOL CHANNEL BASIN

The BCB (Fig. 1) is an exhumed E–W-trending Mesozoic basin. Basin formation started as early as the Permian, with N–S extension causing reactivation of south-dipping Variscan thrusts (Van Hoorn, 1987;

Brooks *et al.*, 1988; Roberts, 1989). Extension and subsidence continued through the Triassic and Jurassic, with E–W-striking normal faults and calcite veins being well exposed on the Somerset coast (Peacock and Sanderson, 1991, 1992, 1994). Evidence for Alpine N–S contraction on the Somerset coast includes E–W-striking thrusts and reactivated normal faults (Peacock and Sanderson, 1992; Dart *et al.*, 1995), and strike-slip faults conjugate about N–S (Peacock and Sanderson, 1992, 1995). E–W-trending folds are related to wall-rock deformation around the E–W-striking normal faults, but were probably tightened during the N–S Alpine compression. NNW-striking faults, e.g. the Sticklepath Fault Zone, appear to date back to the Variscan, and may have been active at various times (Holloway and Chadwick, 1986; Lake and Karner, 1987; Van Hoorn, 1987; Roberts, 1989). Sinistral displacement occurred on these faults during the early Tertiary, so  $\sigma_1$  was approximately NW–SE across the BCB at that time (Van Hoorn, 1987). Dextral displacement occurred during the late Oligocene to Miocene (Arthur, 1989), so  $\sigma_1$  was approximately N–S across the BCB (Van Hoorn, 1987).

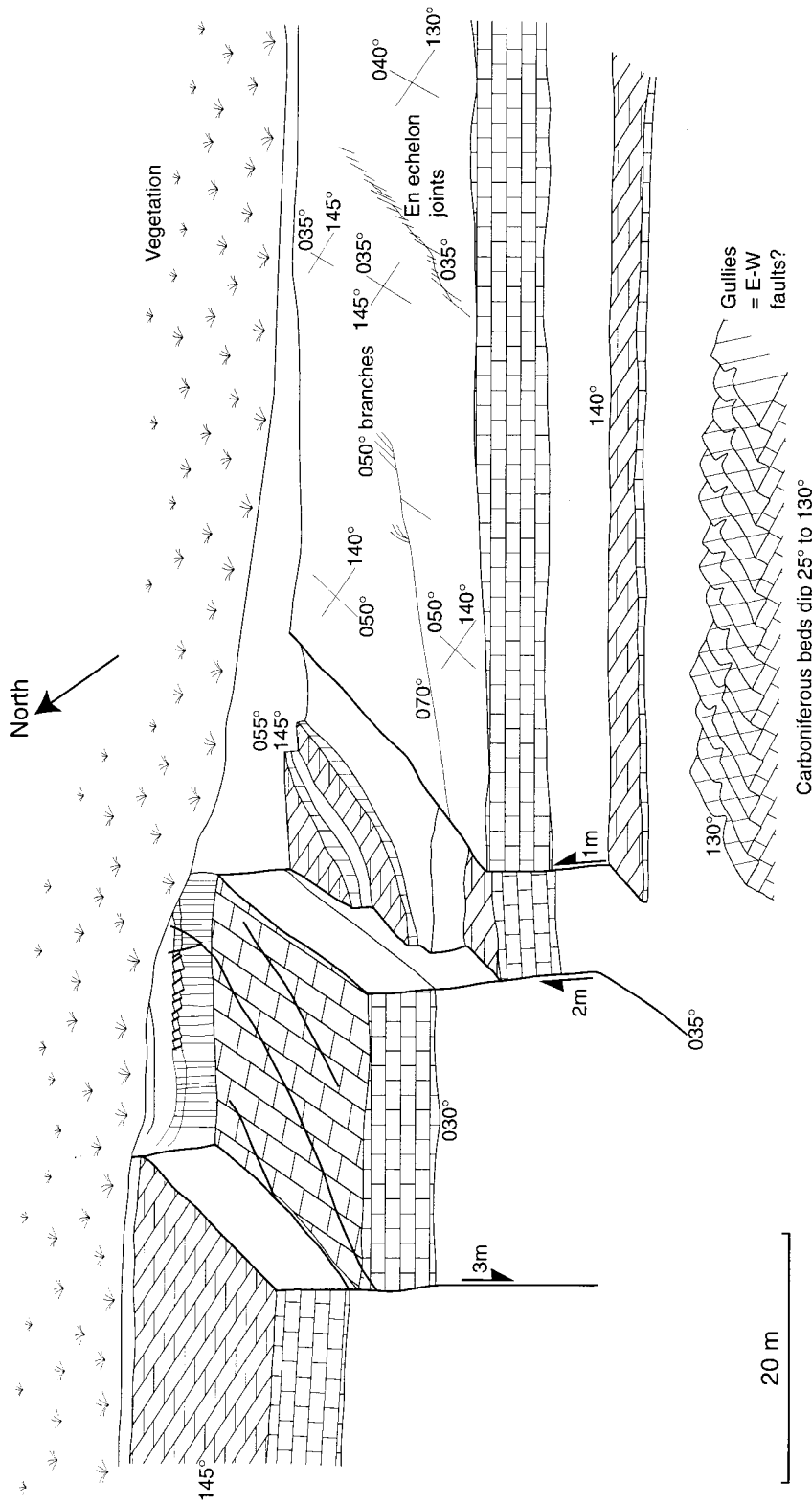


Fig. 4. Schematic view of location 3, Sully Island, showing the faults and joint trends.

## JOINTS AT SULLY ISLAND

A geologic map of Sully Island is shown in Fig. 2. A palaeo-hill of Carboniferous Limestone is exposed on the south coast of Sully Island. There is a thin cover of Triassic conglomerates and sandstones, overlain by terrestrial siltstones, mudstones and limestones.

A SW-plunging syncline has its hinge between Sully Island and the mainland, with beds on the island dipping at about  $5^\circ$  to the northwest. The St Mary's Well Bay Fault Zone (SMWBFZ) strikes about  $160^\circ$  and passes to the east of Sully Island. This fault dips about  $55^\circ$  west and displaces Liassic sediments over the Triassic sediments. The SMWBFZ appears to be part

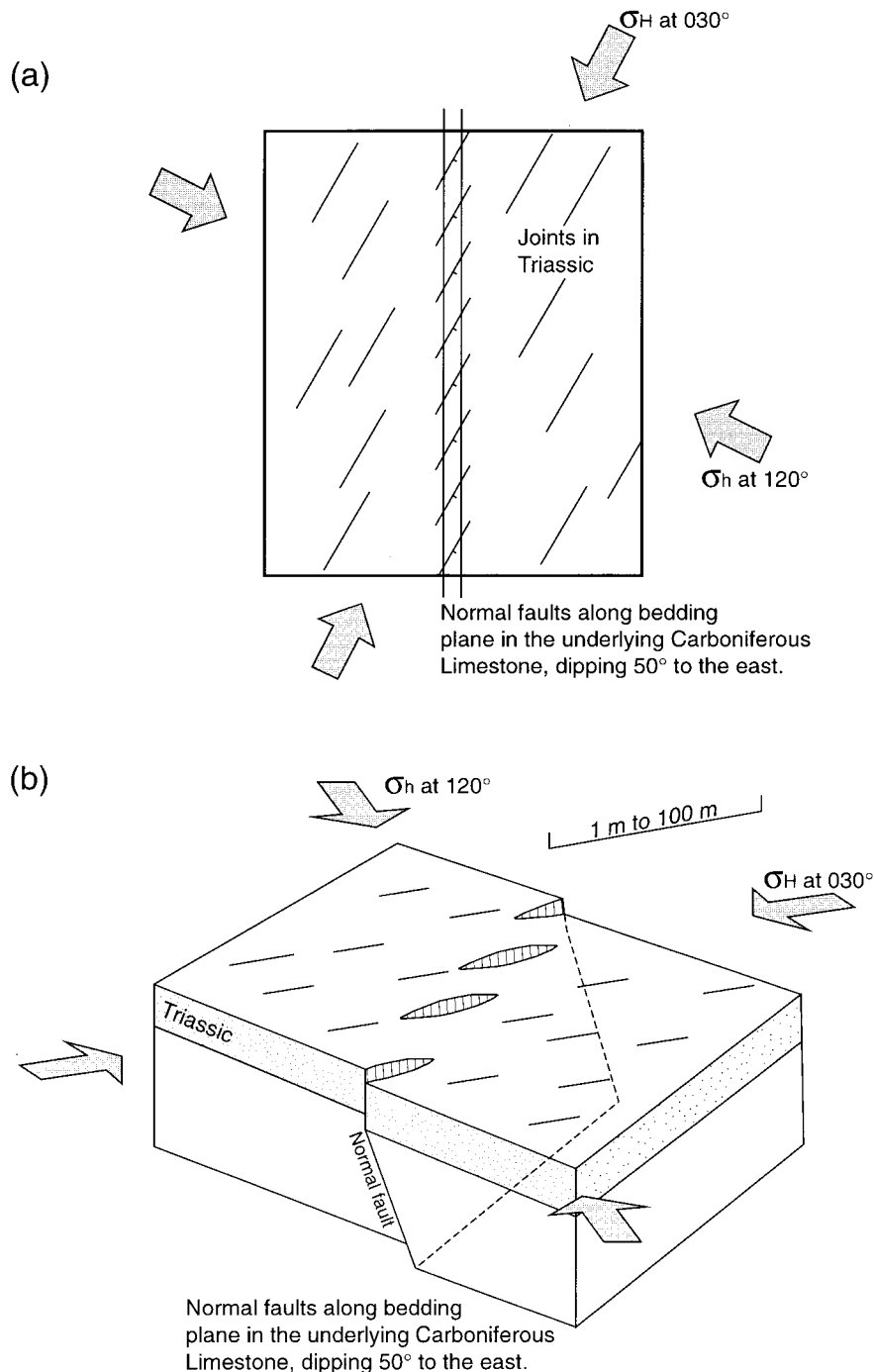


Fig. 5. (a) Plan view and (b) block diagram of a fault along a bedding plane in the Carboniferous rocks, with en échelon joints and faults developed in the overlying Triassic rocks.  $\sigma_H$  was oriented at  $030^\circ$ . The scale bar can be between 1 m and 100 m.

Table 1. Joints east of the syncline axis at Lavernock Point

Bed	Bed thickness	Joint Order	Strike	Comments
11–14				Sets at 010–020°, 125° and 110°.
8 and 10		3	100°	Three sets indicate variations in $\sigma_H$ directions.
		2	080°	
		1	110°	
4–7				Sets at 130°, 110°, 100°, 080° and 005°.
3	0.15 m	4	020°	Non-cross-cutting, orthogonal to the 110° set. Left-stepping array. Abut or curve into 110° joints. Abut against and branch from 130° joints. Right-stepping array.
		3	170°	
		2	110°	
		1	130°	
2	0.11 m	4	Varies	Late stage polygonal joints, indicating isotropic stress. Some abut against 110° joints, implying reactivation. Abut against or cut 160° joints.
		3	160°	
		2	110°	
		1	160°	
1	0.12 m	2	0.15°	Orthogonal to closely-spaced 105° joints. Polygonal, abutting widely spaced 105° joints. > 15 m long. Reaction rims around all three sets.
		2	Varies	
		1	105°	

of a flower structure and may be a reactivated basement fault, having the same trend as major faults in the Carboniferous to the north. It has slickenside lineations which indicate phases of reverse and of dextral displacement. On Sully Island, there is a fault zone striking about 030°, with sub-vertical segments striking approximately N–S, and with throws of 0.5–7 m down to the east. The fracturing at Sully Island is complex and varies between beds. Five locations (Fig. 2) are described, these representing most stratigraphic units and structural settings present.

#### Location 1

A 1-m displacement normal fault follows a Carboniferous Limestone bedding plane, which dips at 50° to the east (Fig. 3). In the red Triassic mudrocks above this fault, there is a sub-vertical fault with a displacement of about 0.6 m down to the east. To the east, a series of NW-dipping normal faults with displacements of up to about 50 mm occur in the lower 3 m of Triassic rocks. Joints in the Triassic mudrocks are vertical and strike 020–030°, with a spacing of 10–20 m. Some curve to become parallel to the NW-dipping normal faults. Some of the joints have calcite fill; these are different from the tectonic calcite veins in the region (*cf.* Peacock, 1991) because the calcite is vuggy, they are longer, thinner and more segmented, and because not all of them are filled by calcite. This

suggests that they did not originate as veins, but as joints which were later mineralized.

#### Location 2

This is about 20 m west of location 1. Similar normal faults occur along beds in the Carboniferous Limestones, also with smaller faults in the overlying Triassic sediments. Sub-vertical 030° striking branch cracks, often filled with vuggy calcite, are often related to the faults. Joints also strike 030°. N–S-trending joint arrays in the conglomerates at the base of the Triassic sediments separate the faults in the Carboniferous from those in the Triassic, with individual segments in the array striking 030°, indicating dextral shear. In the west of the location, two orthogonal joint sets occur. The 120° striking joint set is sub-parallel to the coast, so few are exposed. The 030° striking set is mostly planar, but many are in left-stepping arrays, with oversteps of 10–150 mm. Many have vuggy calcite filling up to 5 mm thick. Some joints which initiated in limestone beds cross into mudrocks, while joints from the mudrocks rarely cross into limestones.

#### Location 3

This location includes two sub-vertical left-stepping faults striking at 030° (Fig. 4). Several NW-dipping

Table 2. Joints west of the syncline axis at Lavernock Point

Bed	Joint order	Strike	Comments
11, 13 and 14	3	Varies	Rare polygonal joints.
	2	170°	Often trail or branch from 010° joints, indicating reactivation.
	1	010°	Not normal to beds, but dip 8° west.
2 and 3			Sets at 160° and 020°, but chronology is unclear.

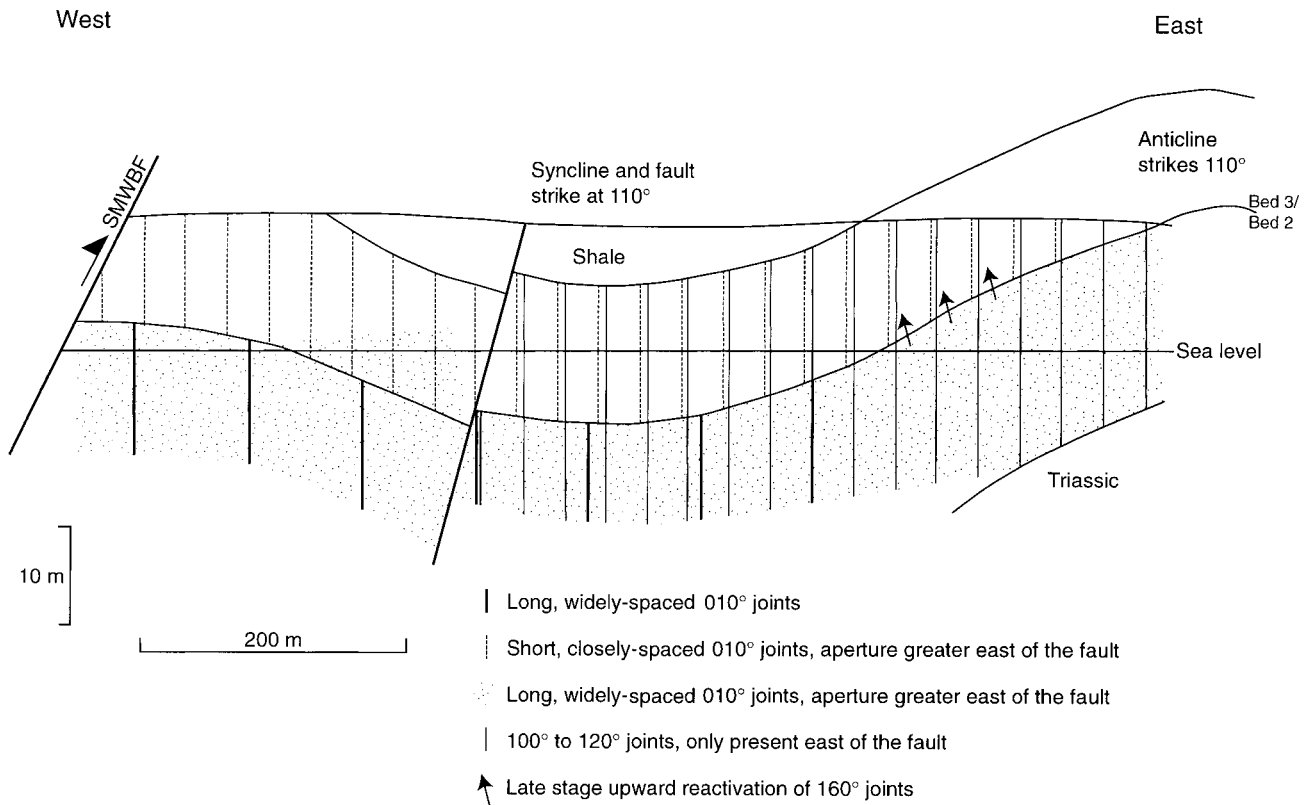


Fig. 6. Schematic cross-section showing the horizontal and vertical zonation of joint sets at Lavernock Point.

faults occur, dying out upwards into vertical 030° striking branch cracks, with some rotation of bedding. Two orthogonal joint sets occur, striking at about 055° and 145°. Between the two main faults, however, the joints strike at 030°. Many joints have vuggy calcite filling, with average widths of about 1.6 mm.

#### Location 4

The 50–100 mm thick carbonaceous siltstones and mudstones have joint strikes mostly of 030° and 040°. The 030° joints are later, and may branch from the terminations of the 040° striking joints. This suggests rotation of  $\sigma_H$  (maximum horizontal stress) from 040° to 030°.

#### Location 5

This location is bounded to the east by one of the 030° striking fault segments, and comprises the upper surface of a silty limestone bed. Joint arrays either strike at 120° and contain segments striking at 140°, or the arrays strike at 140° and contain segments striking at 120°. These joints could be formed by mode III reactivation of underlying joints, with  $\sigma_H$  approximately 130°, i.e. within the bisectrix of the arrays. Right-stepping arrays strike about 060° and contain

segments striking at 040°. Calcite veins in the north of the location strike 030°, but further south, in underlying beds, these are replaced by stylolites which strike at 040°. Polygonal joints pre-date the joint arrays, and appear to have been filled by dolomite before the arrays formed. They cut the bed into polygons, commonly over 5 m diameter.

#### Factors affecting joints at Sully Island

The joints are often arrested at lithological boundaries, with joints in the mudrocks rarely crossing into the limestones. There are also spatial variations in joint patterns. The N–S-striking en échelon faults appear to be controlled by slip along beds in the Carboniferous limestones (Fig. 5). These faults appear to perturb stresses and cause complexity in joint patterns, as at location 3. Minor perturbations in  $\sigma_H$  directions at location 4 may be related to the closure of a syncline to the northeast. The 030° striking joints formed during reactivation of the Carboniferous faults, and formed during the north-northeast or northeast contraction responsible for large-scale reactivation of Carboniferous structures and for the creation of the SMWBFZ during the Alpine compression. Joints orthogonal to the 030° set may be related to relaxation following the contractional event.



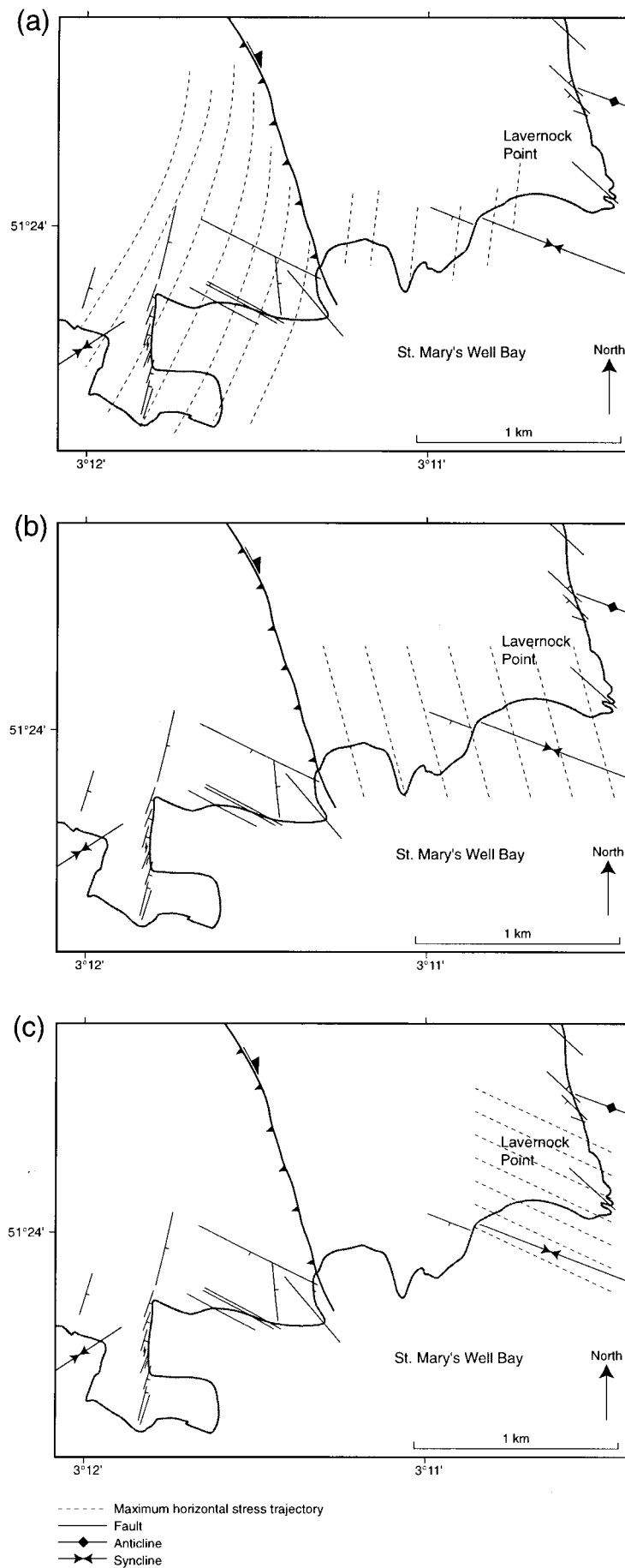


Fig. 7. Maps showing the proposed stress history at Lavernock Point during the formation of the joint sets. (a) Formation of  $010\text{--}020^\circ$  striking joints during Alpine compression. (b) Formation of  $160\text{--}170^\circ$  striking joints, possibly during a decrease in Alpine compression. (c) Formation of  $110\text{--}120^\circ$  striking joints induced by tensile stresses parallel to fold axes.

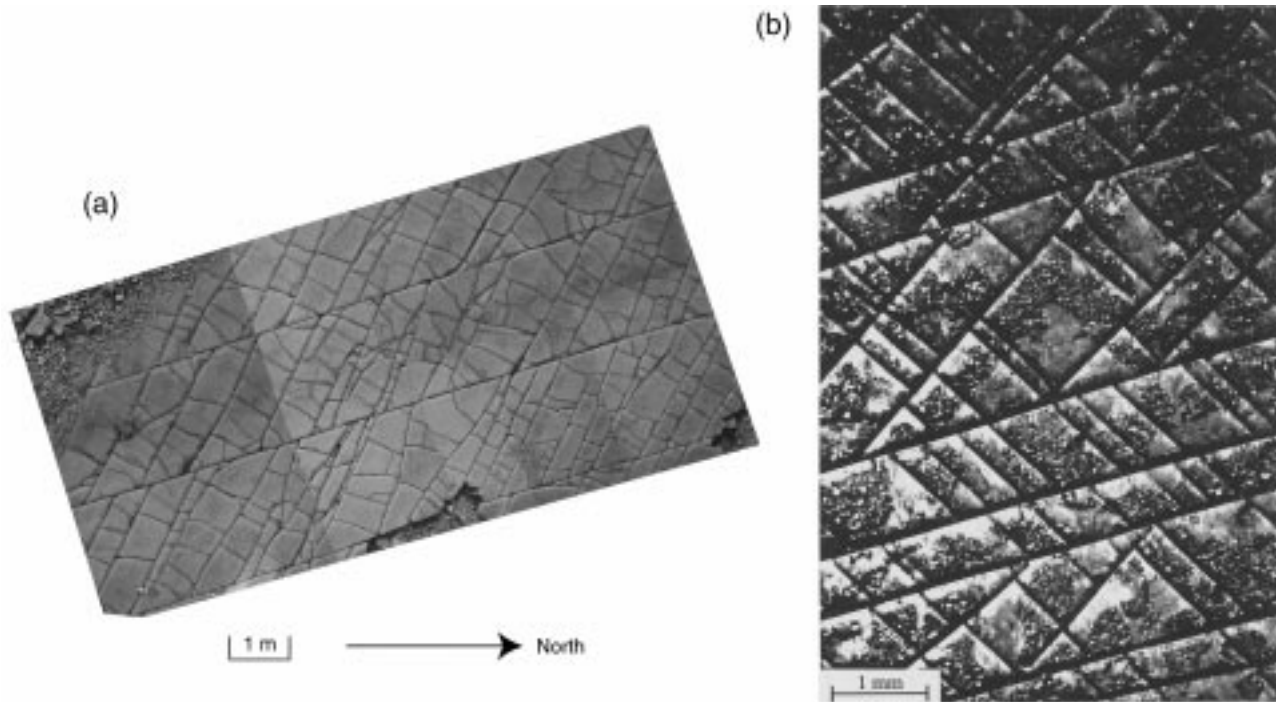


Fig. 8. Examples of joints patterns. (a) A natural joint pattern from Lavernock Point. Long  $160^\circ$  striking joints are present, with abutting more closely-spaced  $110\text{--}120^\circ$  striking joints. (b) A brittle varnish model (Rives *et al.*, 1994) displaying a very similar geometry to (a).

### JOINTS AT LAVERNOCK POINT

Lavernock Point consists of Rheatic and basal Liassic limestones and shales. A syncline plunges to the southeast (Fig. 2), with beds in the east dipping about  $5^\circ$  to the southwest and beds to the west dipping at about  $5^\circ$  to the southeast. To the west, the syncline abuts the SMWBFZ. A normal fault near the syncline axis dips towards  $200^\circ$ , has about 3 m throw in the cliff, and dies out southeast-wards. Calcite veins occur near, and sub-parallel to, the fault. These veins are cut by joints.

Fifteen limestone beds are exposed on the limbs of the syncline. Variations in joint patterns are described in beds 1–14 (Tables 1 & 2), with bed 1 being the lowest and furthest from the syncline. There is no clear relationship between joint spacing and bed thickness. The later joints are typically polygonal if the first set is widely-spaced, or orthogonal to the first set if that set is closely-spaced. This suggests increased modification of the stresses as the spacing decreases. A schematic representation of the joints at Lavernock Point is shown in Fig. 6. The main characteristics of the joint sets are described below:

*010° striking set:* This set occurs in all beds above bed 3. They are mostly shorter than 4 m and are closely-spaced. These are mostly the earliest joints and are often a few degrees from being normal to bedding. They appear to have been closed during the develop-

ment of  $160^\circ$  striking joints, because they are cut by the later  $160^\circ$  striking joints. The  $010^\circ$   $\sigma_H$  direction implied by these joints corresponds with dextral displacement on the SMWBFZ, indicating that the joints formed during the period the fault was active (Fig. 7a). Non-cross-cutting joints perpendicular to the  $010^\circ$  striking set abut, and so also post-date, the  $160^\circ$  striking joints.

*160° striking set:* This set is present below bed 3, and more rarely above. In the east, this set appears to have been reactivated from bed 2 to bed 3. This set does not appear to have been affected by the fault or syncline.  $\sigma_H$  would have been at  $160^\circ$  during development of these joints, and does not appear to have been perturbed. They are unaffected by  $010^\circ$  striking joints, but strongly affect  $100\text{--}120^\circ$  striking joints. There are no joints orthogonal to the  $160^\circ$  striking set, indicating little relaxation or contraction before the  $100\text{--}120^\circ$  striking set. It could be that N–S compression reduced after formation of the  $010^\circ$  striking set and during movement on the SMWBFZ, so  $\sigma_H$  rotated to  $160^\circ$ , which is normal to the fault (Fig. 7b). East of the syncline axis,  $160^\circ$  striking joints in bed 2 appear to have undergone dextral or extensional reactivation, producing left-stepping  $170^\circ$  striking joints in bed 3.

*100–120° striking set:* This set occurs in all the limestone beds east of the normal fault (Fig. 8a). Strike variations are common, with evidence for a temporal

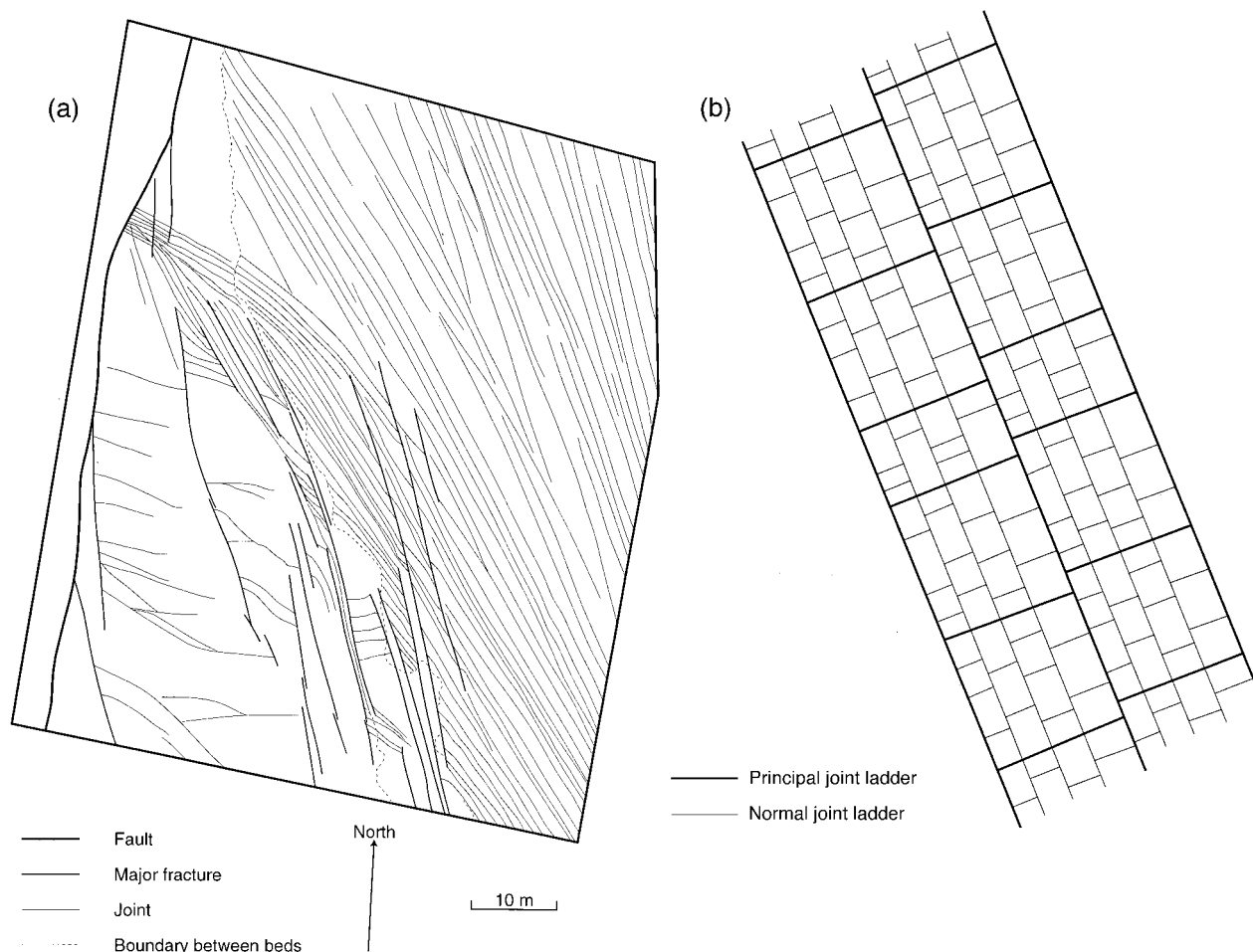


Fig. 9. (a) Map of the western fault zone and major joints in area 1, Nash Point. The direction of joints is indicated, but not the lengths, spacings or exact positions of joints. (b) Map of the ladder pattern of joints at area 1, Nash Point.

sequence from  $120^\circ$  striking joints, then  $100^\circ$  striking joints, then  $110^\circ$  striking joints. Absence of these joints east of the normal fault suggests they are influenced by the fault (Fig. 7c), which perhaps separated areas with different stresses. These joints are sub-parallel to the Alpine-age anticline northeast of Lavernock Point, and the joint apertures increase towards the anticline. This indicates the joints are related to extension in the anticline, and may be pre- or syn-folding. In Fig. 8(a), long  $160^\circ$  striking joints are present, against which more closely-spaced  $110$ – $120^\circ$  striking joints abut. Joints have developed orthogonal to the  $110$ – $120^\circ$  striking joints. A brittle varnish model (Rives *et al.*, 1994) which was subjected to two phases of extension (Fig. 8b) shows a similar geometry to the natural example (Fig. 8a). The first phase was perpendicular to the  $160^\circ$  direction, and the second phase was perpendicular to the  $110^\circ$  direction. The orthogonal joints developed during relaxation.

*Polygonal joints:* These occur in larger blocks and indicate horizontally isotropic effective tension. They may represent thermal contraction in response to

uplift, which may also be responsible for non-cross-cutting perpendicular joints between closely-spaced joints.

## JOINTS AT NASH POINT

This location consists of inter-bedded Liassic limestones and shales, with beds rarely  $>1$  m thick and dipping  $<5^\circ$  to the south. To the east of Nash Point, a  $140^\circ$  striking dextral fault zone occurs, indicating  $\sigma_1$  was approximately N–S. It extends for  $>5$  km to the northwest and is colinear with faults in Carboniferous rocks further northwest. A  $170^\circ$  striking fault zone forms the western boundary of the location, and is exposed for about 2.8 km. This fault zone has sub-horizontal slickenside lineations.

### *Area 1: west of Nash Point*

This area is near the car park at Nash Point Lighthouse. About 150 m width of beach is uncovered at low tide, with five extensive limestone beds occur-

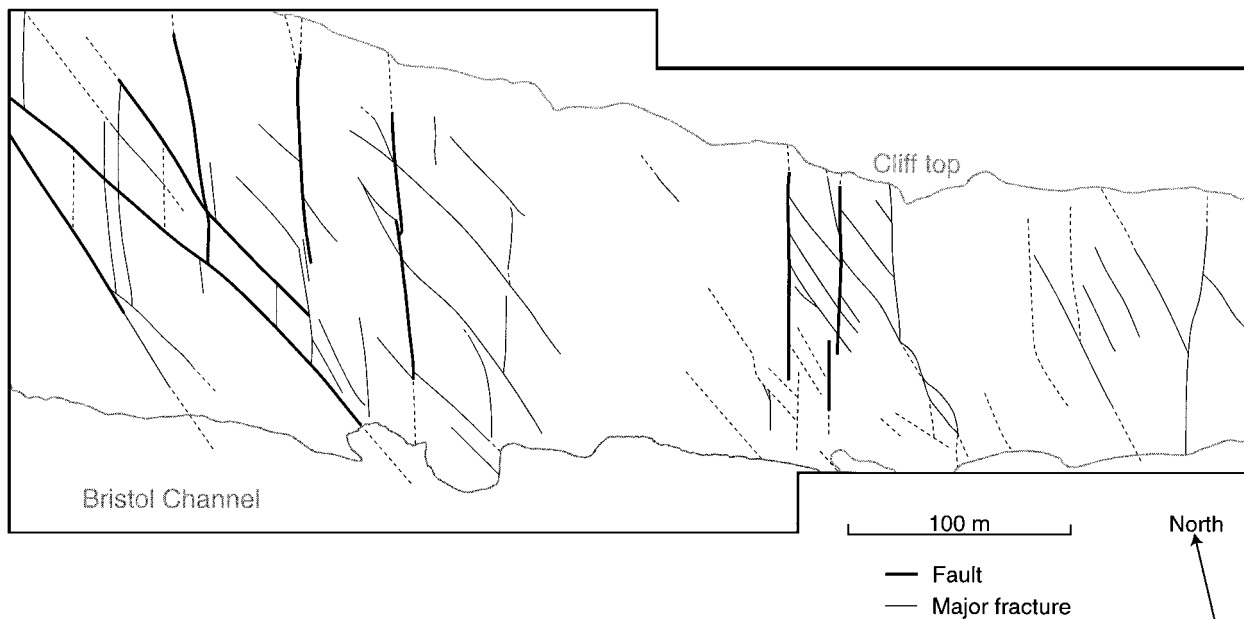


Fig. 10. Map of the faults and main joints in area 2 at Nash Point, about 800 m east of area 1 and about 500 m west of the St Donats fault.

ring. The area is between two fault zones. The western fault zone is vertical, about 10 m wide and contains several segments with normal displacements. One segment shows sub-horizontal slickenside lineations. The eastern fault zone strikes  $170^\circ$ , contains vertical left-stepping segments striking  $170\text{--}180^\circ$ , and has a vertical displacement of about 1.2 m. Calcite veins  $< 10$  mm thick are common. These high density veins (HDVs) pre-date, and are often exploited by, the joints. They strike mostly N–S in area 1, i.e. parallel to the faults. Two groups of orthogonal sets of HDVs occur immediately west of the western fault zone, these striking N–S and E–W, and  $060^\circ$  and  $150^\circ$ .

The joint pattern varies across area 1 (Fig. 9a). In the east, the main set strikes  $155\text{--}160^\circ$ . There is a two-level hierarchy, with  $160^\circ$  joints connected by orthogonal joints to form a ‘ladder’ pattern which crosses between beds. Within these ladders, shorter  $160^\circ$  joints and non-cross-cutting orthogonal joints form a smaller-scale system of ladders (Fig. 9b) which mostly do not cross between beds.

A series of 8–40 m long, 1–10 m spaced predominant  $155\text{--}165^\circ$  striking joints cut across the west of the area. These prominent joints pre-date and often perturb the smaller joints. They show no evidence of shear displacement, and may be perturbed by the western fault zone. Joints in the west are less regular than in the east, and curve to a point on the western fault, where the fault bends. The main joints are mostly perpendicular to the prominent joints, but joints between these main joints show little preferred orientation. Within the triangles between the western fault and

major joints, long joints are almost perpendicular to the major joints. Shorter joints are orthogonal to these long joints, and the remaining rock is cut into polygons. Individual joints rarely connect between different limestone beds.

#### Area 2: east of Nash Point

Area 2 (Fig. 10) is about 800 m east of area 1 and about 500 m west of the St Donats fault. This area shows excellent examples of joint perturbations around faults (Rawnsley *et al.*, 1992, 1997; Petit *et al.*, in review), with one limestone bedding plane being exposed across most of the area. Two fault sets occur, striking at  $000\text{--}010^\circ$  and at  $145^\circ$ . Displacements are less than a few metres, and fault terminations are often exposed. Several major joints occur with the same strikes as these fault sets. Joints are mostly perturbed by the faults and major joints. Three main types of perturbation occur:

1. curving parallel to faults
2. converging towards points on faults (Fig. 11)
3. branching from fault tips.

For a full description, see Rawnsley *et al.* (1992). Small-scale polygons occur between the perturbed joints.

#### Model for joint development at Nash Point (Fig. 12)

High density veins (closely-spaced  $< 10$  mm thick calcite veins) strike  $170\text{--}010^\circ$ , indicating approximately

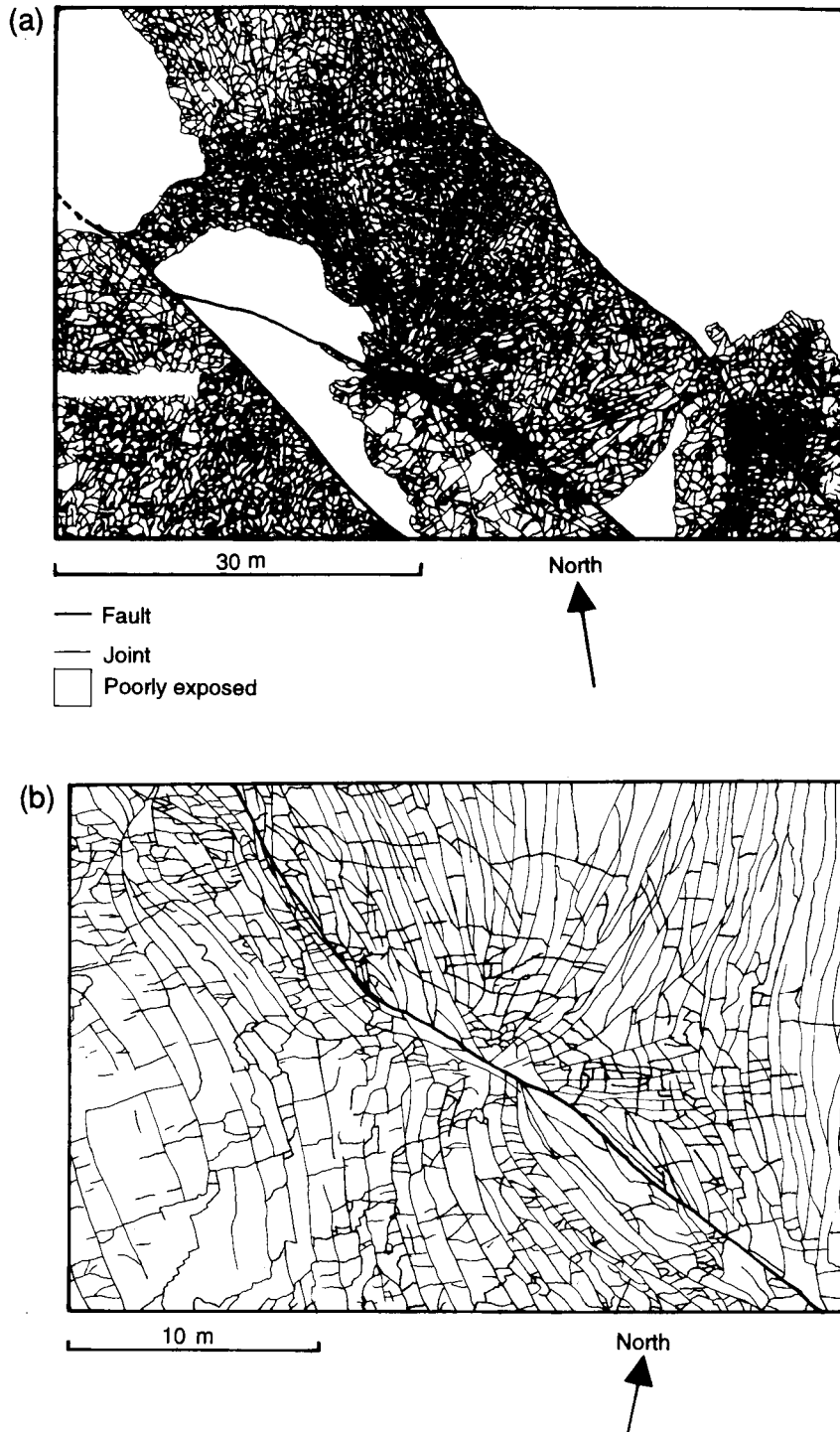


Fig. 11. Line drawings from air photographs of perturbations of joints in area 2, Nash Point. (a) Several points of joint convergence occur along parallel 145° striking faults. Joints mutually cross-cut joints from other points of convergence, and may curve from one point to another. (b) Joint perturbation in an area of about 150 m<sup>2</sup>.

N–S  $\sigma_H$  which is the Alpine compression direction (Fig. 12b). These are followed by the 010–170° striking faults (Fig. 12c). The 010° faults appear to be dextral and the 170° faults appear to be sinistral, so they are conjugate about N–S. The St Donats fault strikes 145°

and is parallel to faults in the Carboniferous to the north, implying it is a Variscan fault which underwent dextral reactivation during the Alpine. Other 145° striking faults in the area may also be reactivated

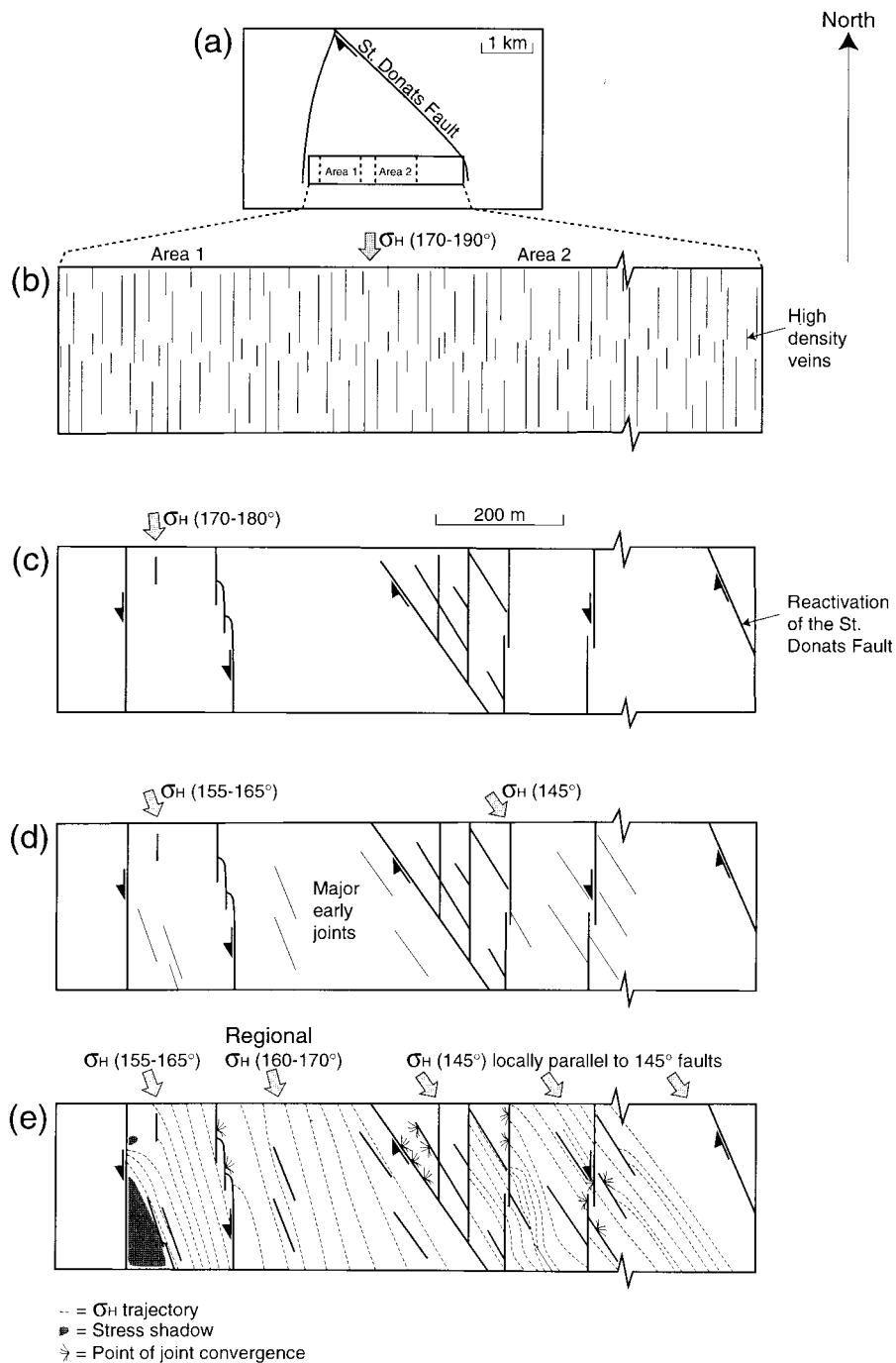


Fig. 12. Schematic maps illustrating the development of joints at Nash Point. (a) Map of the whole area, showing Nash Point Fault and Areas 1 and 2. (b) The high density veins are  $< 1$  mm wide and have spacings of less than a few millimetres. (c) A system of strike-slip faults developed. (d) The major 145° striking joints formed after fault movement ended, when  $\sigma_H$  was perturbed into parallelism with the faults. (e) Joints formed which converge into points on the strike-slip faults.

Variscan structures, or may be connected at depth to the St Donats fault.

The major joints strike 145° and formed when  $\sigma_H$  was perturbed into parallelism with the 145° faults after fault movement ended (Fig. 12d). These non-perturbed joints were followed by perturbed joints, corresponding with a relaxation of the compressive stress

(Fig. 12e). Points of joint convergence resulted from irregularities on the fault planes causing the stress trajectories, and the joints that follow them, to converge (Rawnsley *et al.*, 1992). The  $\sigma_H$  direction in area 1 was 155–165°, except where perturbed by the western fault, with cross-joints forming between the 160° joints. Late

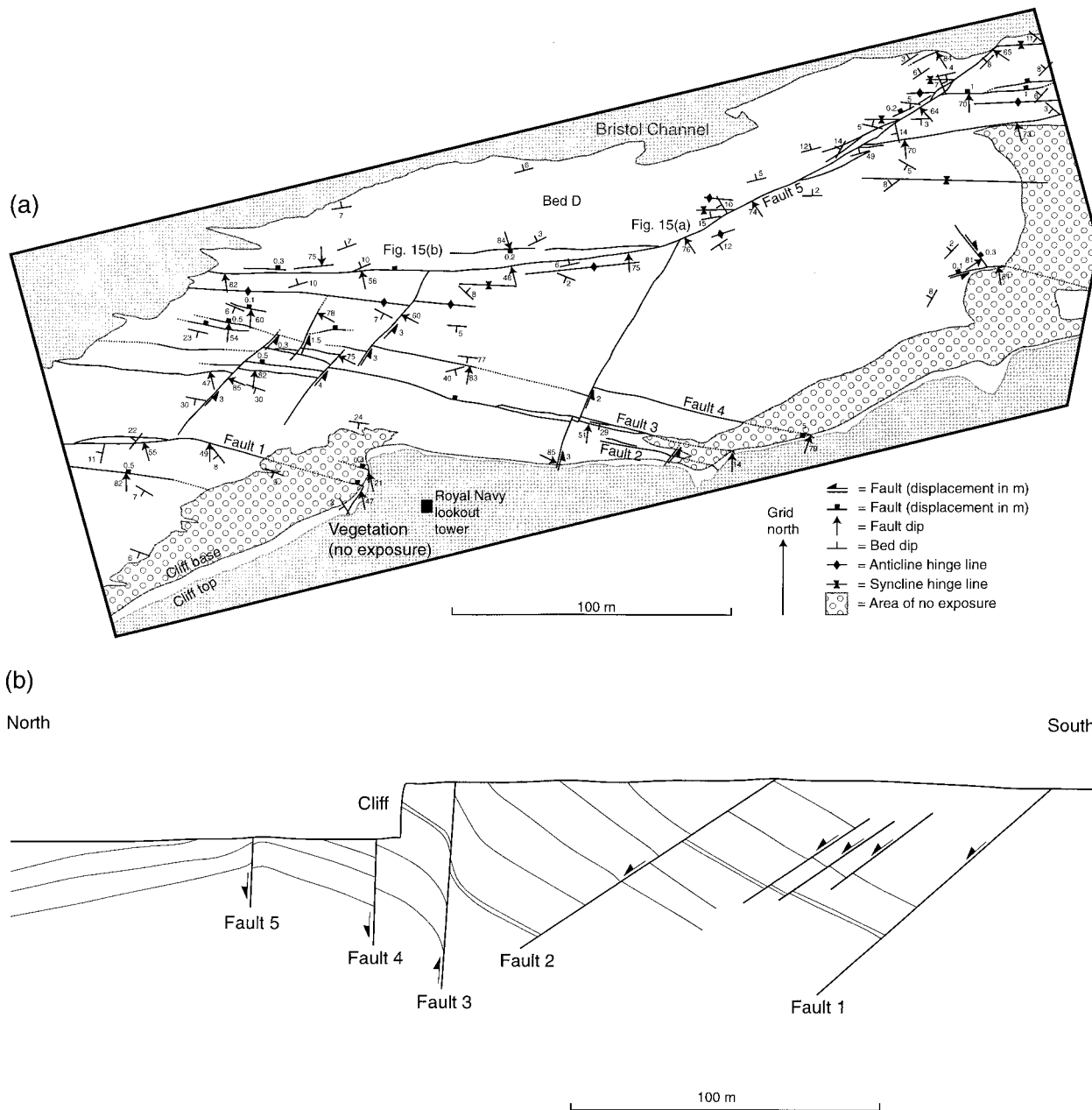


Fig. 13. (a) Map of the area analysed at Lilstock, showing the locations of Fig. 15(a & b). (b) N-S cross-section across Lilstock.

stage polygonal joints may be related to uplift and tensile residual stresses (Petit *et al.*, in review).

### JOINTS AT LILSTOCK

The area between Lilstock and Kilve shows Lias limestones which are usually <0.3 m thick and shales which are usually <2 m thick. A map and cross-section are shown in Fig. 13. An anticline strikes approximately 110–120°, with beds in the south limb dipping

at up to nearly 90°. Most normal faults dip at 30–40° towards about 020°, with throws of up to >40 m. Branch cracks are visible at the tips of some normal faults in cross-section. Calcite veins occur along many of the faults, and indicate initial mode I opening and then shear (Peacock and Sanderson, 1992, Fig. 9). Fault zone F3 shows about 5 m reverse displacement, with adjacent beds becoming nearly vertical. Segments in this zone show both normal and reverse displacement, with some slickenside lineations indicating dextral displacement. Sinistral strike-slip faults strike 040°

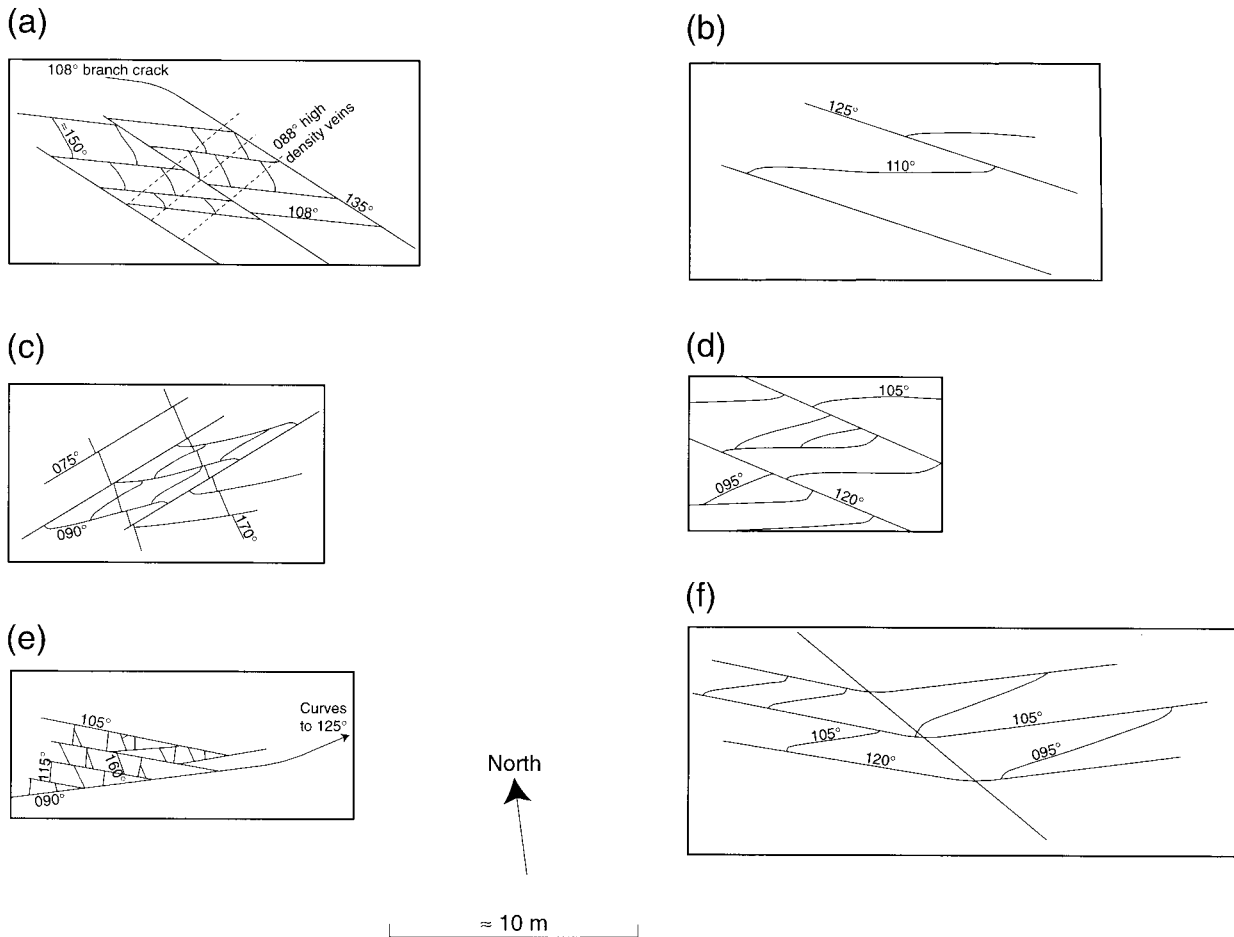


Fig. 14. Examples of different joint patterns at Lilstock. Phase 2 and phase 3 joints strike approximately ESE, while phase 4 joints are the cross-joints.

and displace the normal faults. Fault F5 strikes  $065^\circ$  in the east, curving to  $090^\circ$  in the west, with both sections dipping at  $60\text{--}70^\circ$  northwards. The movement sense is not clear, but the fault zone has an overall normal displacement. Normal fault segments with  $<0.5$  m displacement occur along the  $065^\circ$  striking portion of fault F5.

*Evidence for the age of the joints in the Mesozoic sediments of the Somerset coast*

Evidence that the joints post-date the normal and strike-slip faults includes:

1. The joints are not mineralized, even though there are many veins associated with the faults and the faults themselves are mineralized (e.g. Peacock and Sanderson, 1995). The joint may have been closed again during fault formation, but the absence of veins suggests that the joints cannot be synchronous with fault development.
2. Some joints extend on from the tips of the normal faults. It has been suggested (C. Townsend, personal communication) that this means that the faults formed along pre-existing joints. The faults clearly follow pre-existing veins, which were precursors to the faults (Peacock and Sanderson, 1992), but these veins are cut by the joints. This suggests that the joints follow earlier normal faults, not that the normal faults follow earlier joints.
3. The strike-slip faults cut, so are later than, the normal faults. The joints abut the strike-slip faults but are not displaced by them. They are therefore later than the strike-slip faults, so must be later than the normal faults. Some joints radiate from points along strike-slip faults, showing that these joints must post-date the normal faults. This was interpreted by Rawnsley *et al.* (1992) as being caused by residual stresses on some of the faults influencing later joint development.



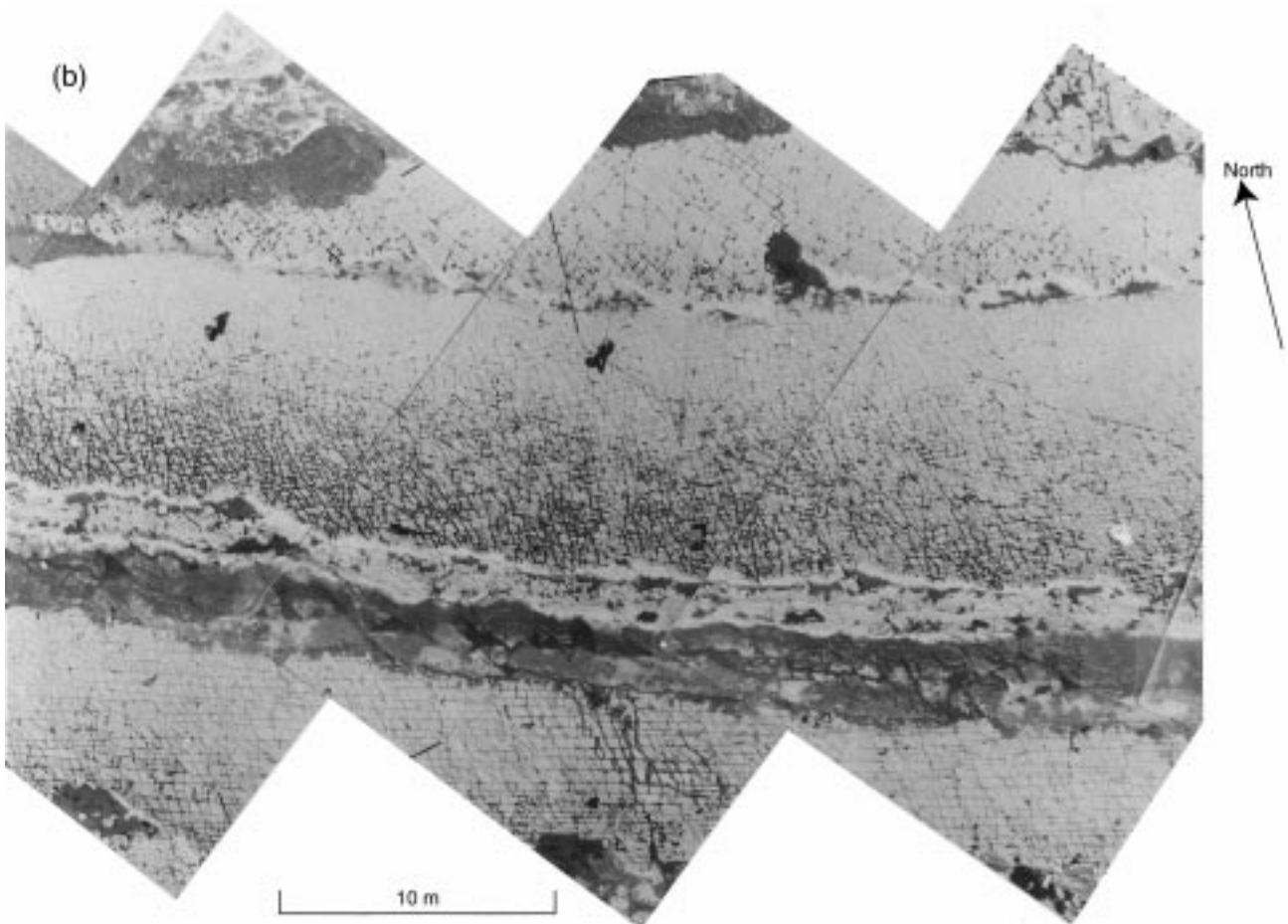
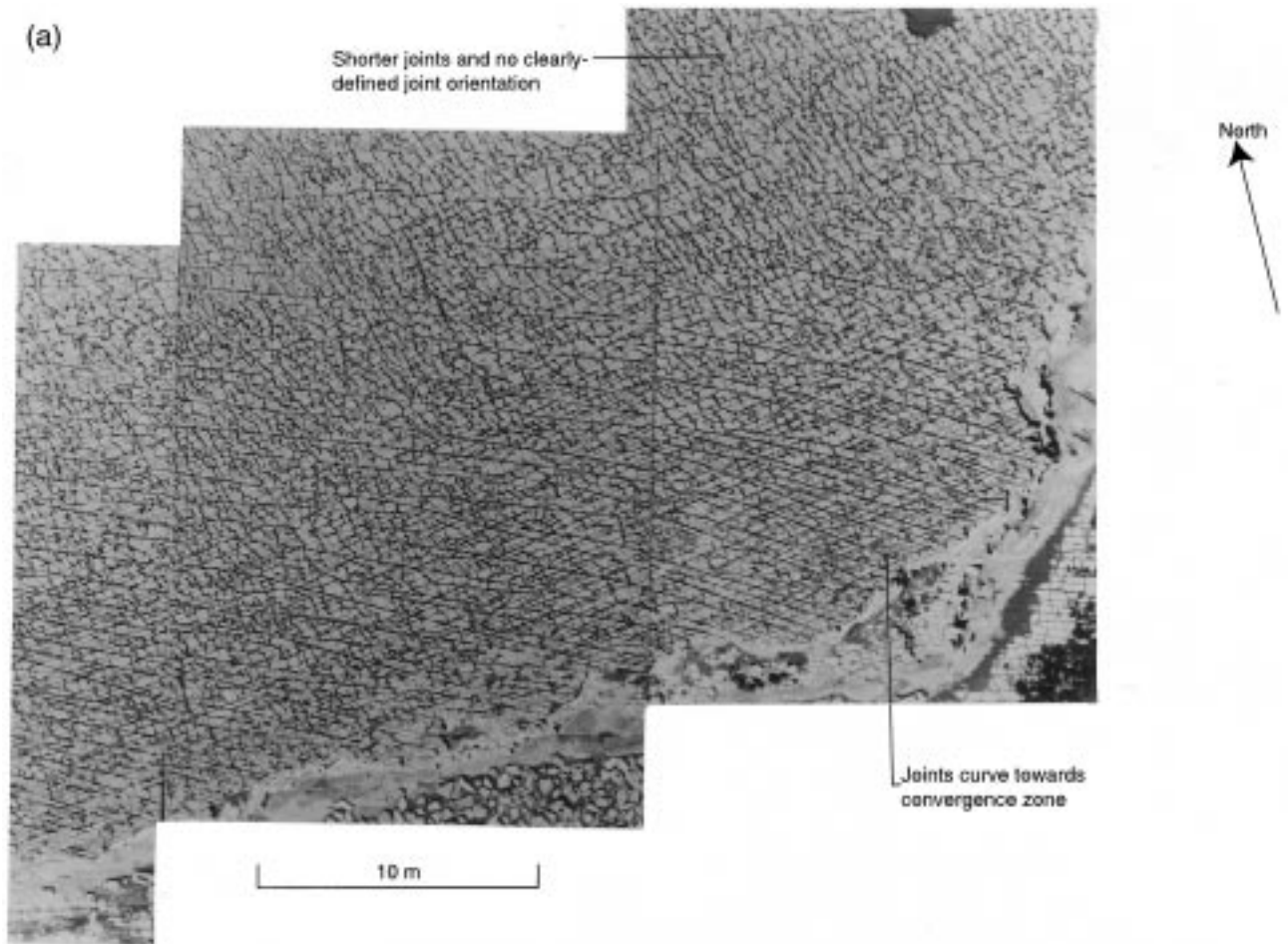
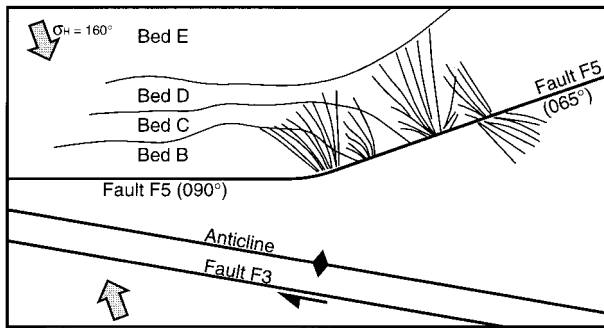
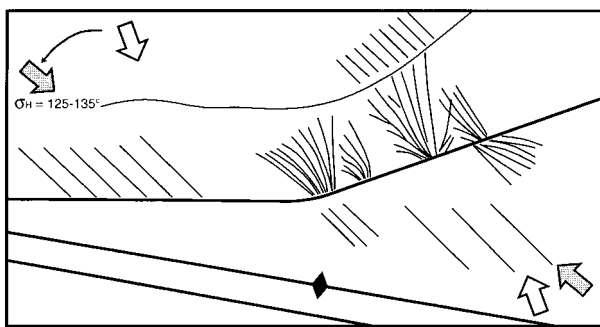


Fig. 15. Details of a photo-mosaic of the south of bed D around fault F5, Lilstock. (a) A zone of joint convergence. (b) Oblique ladders (see pattern in Fig. 14a).

## (a) Phase 2 joints



## (b) Phase 3 joints



## (c) Phase 4 joints

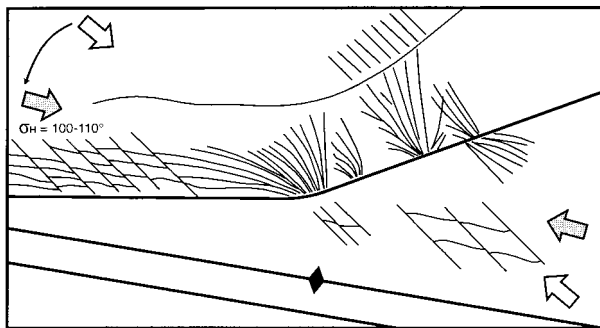


Fig. 16. Maps showing a model for joint development at Lilstock, following dextral reactivation of fault F3. During the relaxation of the regional compression, the  $\sigma_H$  axis rotated anticlockwise to become parallel to the fault. (a) Phase 2 joints, perturbed by the faults. (b) Phase 3 joints, parallel to the  $110^\circ$  striking fold axes. (c) Phase 4 joints, which are cross-joints.

4. The veins related to the strike-slip faults are cut across by joints, which must therefore post-date the normal faults.

*High density veins*

High density veins (thin, closely-spaced calcite veins) appear to be present everywhere in the limestone beds

at Lilstock. In the east, they mostly strike  $090\text{--}110^\circ$ , have average widths of about 0.08 mm, and often have average spacings of  $< 10$  mm. They are often only visible where erosion has enhanced the contrast between the calcite HDVs and the limestone country rock, especially around the edges of joints. In thin section, they can be seen to persist throughout the rock, and are often en échelon. HDVs either pass through the fault-related calcite veins, or are slightly deviated by them. The HDVs are not perturbed by joints, and some joints may follow HDVs. In the west of the area, the HDVs strike  $082\text{--}088^\circ$  and have an average spacing of about 0.2 m. Most calcite has been removed, with oxidization fronts about 30 mm wide. In the cliff, the HDVs strike about  $110^\circ$  and dip at about  $80^\circ$  more steeply to the north than the bedding.

*Joint patterns*

Examples of joint patterns are shown in Figs 14 and 15. Few joints cut between limestone beds, and adjacent limestone beds often have different joint orientations and chronologies. Alternatively, adjacent limestones can have similar patterns but different spacings. There are four main joint sets:

1. converging joint zones
2. oblique ladders
3. left-stepping arrays
4. isotropic joints.

At least three main zones of converging joints occur along the  $065^\circ$  striking section of fault F5, one of which is shown in Fig. 15(b) (also see Swaby and Rawnsley, 1997, fig. 6). They are elongated in a  $140\text{--}180^\circ$  direction. Joint spacing decreases slightly towards the centre of the convergence as the joints curve towards the fault. These converging joints are the longest at Lilstock. Oblique ladders in a  $095\text{--}135^\circ$  direction occur in all limestone beds within about 30 m of fault F3 (Loosveld and Franssen, 1992). They normally young in an anticlockwise sense (i.e.  $135^\circ$  joints are the oldest and  $095^\circ$  joints are the youngest), forming oblique ladders. Left-stepping arrays trend  $160\text{--}170^\circ$  between two zones of convergent joints, the arrays having spacings of about 15 m. Joints with little preferred orientations also occur between zones of convergent joints and can cover extensive areas. Later joints are usually perpendicular and non-cross-cutting to the four main groups. Most joints appear to have impeded later joints, suggesting they remained open during later joint development. Later joints often curve to become normal to the joints they abut. Limestones appear to contain more joints than the shales. Joints

Table 3. Summary of the main deformation events in the Triassic and Liassic exposures around the BCB. It is acknowledged that many of the proposed ages are based on inconclusive evidence, and that further work is needed on dating the joints

Age	Event	Type of structure	Locations
Late or Post Miocene	Progressive relaxation of N–S Alpine compression	Joint phase 5: polygonal joints	All locations
		Joint phase 4: cross-joints	All locations
		Joint phase 3: rotate to parallel with 110° folds	Lavernock (130–105°) and Lilstock (135–090°)
		Joint phase 2: perturbed by faults and phase 1 joints	Nash Point and Lilstock
		Joint phase 1: sub-parallel to regional compression	Nash Point, Lavernock and Lilstock (160–170°)
Late Oligocene to Miocene	Alpine N–S compression	N–S faults	Nash Point
		040° faults	Lilstock
		Reactivation	SMWBFZ
		≈N–S pre-rupture HDVs	Nash Point, Lavernock
Late Cretaceous to	N–S extension	Reactivation	SLFZ
		E–W HDVs?	Nash Point, Lilstock
Jurassic to Early Cretaceous Oligocene	N–S extension	Normal faults	Lavernock, Lilstock
		Reactivation	SLFZ
		E–W HDVs?	Nash Point, Lavernock

often cut from the limestones into the shales, suggesting joint initiation in the limestones.

#### *Model for joint development at Lilstock*

A model for fracturing at Lilstock is shown in Fig. 16. The normal faults developed during the Mesozoic development of the BCB (e.g. Peacock and Sanderson, 1991). They indicate that  $\sigma_1$  was sub-vertical and that  $\sigma_3$  was at about 010°. The low dips of these faults may be due to tilt of bedding towards the south. Fault F3 initiated as a normal fault, but with reverse and dextral phases of (Alpine) reactivation indicating  $\sigma_1$  was approximately NW–SE to N–S. A similar stress system may have caused the 040° striking sinistral faults. The decrease in spacing and increase in aperture of the HDVs towards fault F5, and the parallelism between the HDVs and normal faults, indicates a relationship. The cross-cutting of calcite veins by HDVs could indicate the HDVs post-date the normal faults.

The joints post-date the faults and the HDVs. They are often strongly perturbed by faults and often follow HDVs. Convergent points on F5 are caused by stress concentrations, as at Nash Point. These concentrations often appear to be limestone–limestone contacts across the fault plane. Northwesterly elongations of these zones indicate that  $\sigma_H$  was NW–SE. The widely-spaced 160–170° striking joints may have formed in this stress system.  $\sigma_H$  then rotated anticlockwise, creating joints with progressively more E–W strikes, producing the widely-spaced 125–135° striking joints and then the 110° striking joints (Fig. 16). Rotation of  $\sigma_H$  was

stronger near faults F3 and F5. The initial NW–SE  $\sigma_H$  direction suggests joint formation during reduction of the Alpine compressive stress. Anticlockwise rotation of  $\sigma_H$  was related to relaxation of compression, with  $\sigma_H$  rotating towards parallelism with the earlier folds and normal faults. Joints are normal to bedding but post-date the fold because flexure is related to the veins, which are cut by joints. Joints striking 110–120° are common on the Somerset coast and are related to stress relaxation around the reactivated normal faults and the folds.

The latest, isotropic joints are related to biaxial effective tension in the plane of bedding, especially in ‘shadow zones’ between convergence points. Between the convergent zones, an almost isotropic joint pattern was produced by a low horizontal stress differential. Impedance of later joints by earlier joints indicates they were always open.

#### **MODEL FOR FRACTURING IN THE BRISTOL CHANNEL BASIN**

The joint patterns at the four locations in the BCB suggest the joints all post-date the HDVs and the faults (Table 3). The joints (e.g. Fig. 14) appear to result from five main phases:

Phase 1: These are sub-parallel to a regional Alpine compression direction (about 160–170°), and are almost unperturbed by faults. At Nash Point, the faults started to perturb the stress during the development of phase 1 joints, i.e. there is a transition from phase 1 to phase 2 joints. Phase 1 joints were reactivated after phase 3 at Lavernock.

Phase 2: These are perturbed by faults and by phase 1 joints. The phase 2 joints followed the perturbed stress trajectories, and curved towards points of stress concentration along fault surfaces, e.g. at fault bends. The transition from non-perturbed (phase 1) to perturbed (phase 2) joints reflects a decrease in the regional compression and increasing residual tensile stress (Petit *et al.*, in review). This phase is absent where no faults are present, as at Lavernock.

Phase 3: At Lavernock and Lilstock, it appears that phases 1 and 2 (where present) are replaced by phase 3 joints, which are parallel to the 110° striking fold axes. These joints cut the veins which formed during folding, and result from the relaxation of the Alpine compressional stresses within the folds. Phase 3 joints typically rotated anticlockwise through time to become parallel to the fold axes, perhaps demonstrating the reduction of the regional influence. This phase is absent where there are no folds, as at Nash Point.

Phase 4: This phase consists of cross-joints.

Phase 5: This phase consists of polygonal joint patterns. Phases 4 and 5 both occur at all of the locations studied. They are related to relaxation or contracting of the rock at a late stage. Lorenz and Finley (1991) describe an absence of cross-joints with depth in Colorado.

This model applies well to the observed Liassic exposures. It is possible, however, that the joint pattern in the unexposed centre of the BCB is significantly different from those exposed around the edges of the basin.

## CONCLUSIONS

Detailed analysis of joints at four locations around the Bristol Channel Basin (BCB) indicates the following:

- The joints in Mesozoic sediments of the BCB post-date the faults. The joints are not mineralized, but cut the veins which are related to joint formation. The joints abut, but are not displaced by, the latest (strike-slip) faults.
- The joints within the BCB formed during the decline of Alpine compressional stresses. Joint formation appears to have occurred in five main phases. Phase 1 follows a regional direction, phase 2 is fault-perturbed and phase 3 is fold-related. Phases 4 and 5 are related to relaxation or contraction.
- Each phase of joints shows characteristic patterns, which can be described by such features as orientation, length, spacing and aperture. Joints within thin (<0.05 m) limestone beds are relatively closely spaced, but otherwise joint spacing is only vaguely proportional to bed thickness.

- Other factors influencing joint development in the BCB include the reactivation of joints at a late stage between beds (Lavernock and Lilstock) and the slip of bedding planes in the basement rocks (Sully Island).

*Acknowledgements*—Fieldwork for this paper was sponsored by Shell EMR Agreement 11104463, under the supervision of J.-P. Petit at the University of Montpellier. DCP was sponsored by a NERC ROPA award to R. Knipe. T. Engelder, R. Lisle and C. Townsend are thanked for their careful reviews.

## REFERENCES

- Arthur, M. J. (1989) The Cenozoic evolution of the Lundy pull-apart basin into the Lundy rhomb horst. *Geological Magazine* **126**, 187–198.
- Brooks, M., Trayner, P. M. and Trimble, T. J. (1988) Mesozoic reactivation of Variscan thrusting in the Bristol Channel area, U.K. *Journal of the Geological Society of London* **145**, 439–444.
- Dart, C. J., McClay, K. and Hollings, P. N. (1995) 3D analysis of inverted extensional fault systems, southern Bristol Channel Basin, U.K., in *Basin Inversion*, eds J. G. Buchanan and P. G. Buchanan, pp. 363–413. Geological Society, London, Special Publication, **88**.
- Engelder, T. and Oertel, G. (1985) Correlation between abnormal pore pressure and tectonic jointing in the Devonian Catskill delta. *Geology* **13**, 863–866.
- Hancock, P. L. (1991) Determining contemporaneous stress directions from neotectonic joint systems. *Philosophical Transactions of the Royal Society of London* **A337**, 29–40.
- Holloway, S. and Chadwick, R. A. (1986) The Sticklepath–Lustleigh fault zone: Tertiary sinistral reactivation of a Variscan dextral strike-slip fault. *Journal of the Geological Society of London* **143**, 477–452.
- Lake, S. D. and Karner, G. D. (1987) The structure and evolution of the Wessex Basin, southern England: an example of inversion tectonics. *Tectonophysics* **137**, 347–378.
- Loosveld, R. J. H. and Franssen, R. C. M. W. (1992) Extensional vs shear features: implications for reservoir characterisation. *Society of Petroleum Engineers* **25017**, 23–30.
- Lorenz, J. C. and Finley, S. J. (1991) Regional fractures I: a mechanism for the formation of regional fractures at depth in flat-lying reservoirs. *Bulletin of the American Association of Petroleum Geologists* **75**, 1714–1737.
- Peacock, D. C. P. (1991) A comparison between the displacement geometries of veins and normal faults at Kilve, Somerset. *Proceedings of the Ussher Society* **7**, 363–367.
- Peacock, D. C. P. and Sanderson, D. J. (1991) Displacements, segment linkage and relay ramps in normal fault zones. *Journal of Structural Geology* **13**, 721–733.
- Peacock, D. C. P. and Sanderson, D. J. (1992) Effects of layering and anisotropy on fault geometry. *Journal of the Geological Society of London* **149**, 793–802.
- Peacock, D. C. P. and Sanderson, D. J. (1994) Geometry and development of relay ramps in normal fault systems. *Bulletin of the American Association of Petroleum Geologists* **78**, 147–165.
- Peacock, D. C. P. and Sanderson, D. J. (1995) Strike-slip relay ramps. *Journal of Structural Geology* **17**, 1351–1360.
- Rawnsley, K. D. (1990) The influence of joint origin on engineering properties. Unpublished PhD thesis. University of Leeds, U.K.
- Rawnsley, K. D., Rives, T., Petit, J.-P., Hencher, S. R. and Lumsden, A. C. (1992) Joint development in perturbed stress fields near faults. *Journal of Structural Geology* **14**, 939–951.
- Rawnsley, K. D., Auzias, V., Petit, J.-P. and Rives, T. (1997) Predicting fracture orientations around horizontal wells using stress trajectory models. *Petroleum Geoscience* **3**, 145–152.

- Rives, T., Rawnsley, K. D. and Petit, J.-P. (1994) Analogue simulation of natural orthogonal joint set formation in brittle varnish. *Journal of Structural Geology* **16**, 419–429.
- Roberts, D. G. (1989) Basin inversion in and around the British Isles. In *Inversion Tectonics*, eds M. A. Cooper and G. D. Williams, pp. 131–150. Geological Society Special Publication, **44**.
- Swaby, P. A. and Rawnsley, K. D. (1997) An interactive 3D fracture-modeling environment. *Society of Petroleum Engineers* **9**, 88–92.
- Van Hoorn, B. (1987) The south Celtic Sea/Bristol Channel basin: origin, deformation and inversion history. *Tectonophysics* **137**, 309–334.